

# Dysregulation of lipolysis and lipid metabolism in visceral and subcutaneous adipocytes by high-fat diet: role of ATGL, HSL, and AMPK

Mandeep P. Gaidhu, Nicole M. Anthony, Prital Patel, Thomas J. Hawke and Rolando B. Ceddia

*Am J Physiol Cell Physiol* 298:961-971, 2010. First published Jan 27, 2010;  
doi:10.1152/ajpcell.00547.2009

---

## You might find this additional information useful...

---

This article cites 47 articles, 22 of which you can access free at:

<http://ajpcell.physiology.org/cgi/content/full/298/4/C961#BIBL>

Updated information and services including high-resolution figures, can be found at:

<http://ajpcell.physiology.org/cgi/content/full/298/4/C961>

Additional material and information about *AJP - Cell Physiology* can be found at:

<http://www.the-aps.org/publications/ajpcell>

---

This information is current as of July 30, 2010 .

# Dysregulation of lipolysis and lipid metabolism in visceral and subcutaneous adipocytes by high-fat diet: role of ATGL, HSL, and AMPK

Mandeep P. Gaidhu,<sup>1</sup> Nicole M. Anthony,<sup>1</sup> Prital Patel,<sup>1</sup> Thomas J. Hawke,<sup>1,2</sup> and Rolando B. Ceddia<sup>1</sup>

<sup>1</sup>Muscle Health Research Centre, York University, Toronto; and <sup>2</sup>Pathology and Molecular Medicine, McMaster University, Hamilton, Canada

Submitted 15 December 2009; accepted in final form 25 January 2010

**Gaidhu MP, Anthony NM, Patel P, Hawke TJ, Ceddia RB.** Dysregulation of lipolysis and lipid metabolism in visceral and subcutaneous adipocytes by high-fat diet: role of ATGL, HSL, and AMPK. *Am J Physiol Cell Physiol* 298: C961–C971, 2010. First published January 27, 2010; doi:10.1152/ajpcell.00547.2009.—This study investigated the molecular mechanisms by which a high-fat diet (HFD) dysregulates lipolysis and lipid metabolism in mouse epididymal (visceral, VC) and inguinal (subcutaneous, SC) adipocytes. Eight-weeks of HFD feeding increased adipose triglyceride lipase (ATGL) content and comparative gene identification-58 (CGI-58) expression, whereas hormone-sensitive lipase (HSL) phosphorylation and perilipin content were severely reduced. Adipocytes from HFD mice elicited increased basal but blunted epinephrine-stimulated lipolysis and increased diacylglycerol content in both fat depots. Consistent with impaired adrenergic receptor signaling, HFD also increased adipose-specific phospholipase A<sub>2</sub> expression in both fat depots. Inhibition of E-prostanoid 3 receptor increased basal lipolysis in control adipocytes but failed to acutely alter the effects of HFD on lipolysis in both fat depots. In HFD visceral adipocytes, activation of adenylyl cyclases by forskolin increased HSL phosphorylation and surpassed the lipolytic response of control cells. However, in HFD subcutaneous adipocytes, forskolin induced lipolysis without detectable HSL phosphorylation, suggesting activation of an alternative lipase in response to HFD-induced suppression of HSL in VC and SC adipocytes. HFD also powerfully inhibited basal, epinephrine-, and forskolin-induced AMP kinase (AMPK) activation as well peroxisome proliferator-activated receptor gamma coactivator-1 $\alpha$  expression, citrate synthase activity, and palmitate oxidation in both fat depots. In summary, novel evidence is provided that defective adrenergic receptor signaling combined with upregulation of ATGL and suppression of HSL and AMPK signaling mediate HFD-induced alterations in lipolysis and lipid utilization in VC and SC adipocytes, which may play an important role in defective lipid mobilization and metabolism seen in diet-induced obesity.

adipose tissue; adipose triglyceride lipase; hormone-sensitive lipase; AMP kinase

WHITE ADIPOSE TISSUE (WAT) plays an important role in regulating whole body energy homeostasis. One of its major roles is to release fatty acids (FAs) under conditions of negative energy balance or prolonged exercise to provide energy for peripheral tissues. The molecular machinery involved in triacylglycerol (TAG) breakdown and FA release works in an orderly and regulated fashion, conferring to WAT the capacity to respond to various feeding conditions and to the energy demands of the body. Importantly, conditions that lead to overeating and obesity disrupt normal regulation of WAT lipolysis. In fact, basal lipolysis has repeatedly been reported as

elevated, whereas catecholamine-induced lipolysis is suppressed in obese humans and rodents (26). The classical mechanism to explain this condition is centered on the fact that the largely expanded WAT of obese subjects becomes resistant to insulin, impairing the major lipogenic and antilipolytic effects of this hormone (4, 37, 40). Obesity develops under conditions of chronic energy surplus, indicating that visceral (VC) and subcutaneous (SC) adipocytes must be able to deal with large amounts of lipids being delivered to the WAT. In this scenario, the ability of adipocytes to handle excess lipids via alterations in FA metabolism may play an important role in the adaptive responses of the WAT to obesity. Importantly, obesity is invariably accompanied by increased circulating levels of nonesterified fatty acids (NEFAs) (4–6, 40), indicating that the regulation of energy storage and mobilization of FAs from VC and SC adipocytes is defective. Although literature exists describing the differences between VC and SC fat depots with regard to eliciting distinct lipolytic rates (9, 30, 42), the cellular and molecular mechanisms responsible for these depot-specific characteristics still remain to be elucidated. This is particularly important because it is the excessive accumulation of VC adipose tissue (visceral obesity) that has been strongly correlated with the development of insulin resistance and type 2 diabetes (4, 25). In this scenario, unraveling the molecular mechanisms involved in dysregulation of lipolysis and lipid metabolism in VC and SC WAT in obesity may be of great therapeutic relevance.

Lipolysis in the WAT of humans and rodents is regulated in a step-wise fashion by adipose triglyceride lipase (ATGL), hormone-sensitive lipase (HSL), and monoacylglycerol lipase (MAGL) (4, 27, 28). The current model is that ATGL initiates lipolysis by cleaving the first FA from TAG and then HSL and MAGL act on diacylglycerol (DAG) and monoacylglycerol, respectively, releasing two additional FAs and one glycerol molecule (27). Therefore, the orchestrated activation of ATGL, HSL, and MAGL seems to be required for complete lipolysis to occur in adipocytes. Binding of agonists to the  $\beta$ -adrenergic receptors, coupled to adenylyl cyclase via the stimulatory G protein, leads to an increase in cAMP and activation of protein kinase A (PKA) (4, 15). In rat HSL, PKA phosphorylates serine residues 563, 659, and 660 (2, 4, 39), leading to translocation of HSL to the lipid droplet and to great enhancement of lipolysis. Phosphorylation of perilipin A, a protein associated with the lipid droplet, by PKA has also been demonstrated to be necessary for activation of HSL and for catecholamine-induced lipolysis to occur. Conversely, the cellular energy sensor AMP-activated protein kinase (AMPK) has been demonstrated to phosphorylate serine-565 of HSL, which prevents PKA-mediated phosphorylation of this enzyme and impairs catecholamine-stimulated lipolysis (19). In this con-

Address for reprint requests and other correspondence: R. B. Ceddia, Muscle Health Research Centre-York Univ., 4700 Keele St., Toronto, ON, Canada M3J 1P3 (e-mail: roceddia@yorku.ca).

text, AMPK has been proposed to lower the release of FAs into the circulation, which could help prevent lipotoxicity in peripheral tissues as well as reduce the costly process of re-esterifying FAs in the WAT (3, 17, 20). ATGL activity is also stimulated by catecholamines, but the molecular mechanism(s) underlying this effect is unknown. Although ATGL can be phosphorylated on serine residues 404 and 428 by a yet unidentified kinase, this does not seem to affect the activity of this lipase. There is compelling evidence that the protein comparative gene identification-58 (CGI-58) drastically enhances ATGL-mediated TAG hydrolysis without affecting HSL activity (29). Under basal conditions, CGI-58 is also localized to the lipid droplet in association with perilipin A (21, 29, 38). Upon hormonal stimulation, PKA phosphorylates perilipin A at serine residues 492 and 517, resulting in CGI-58 dissociation (22). Once dissociated, CGI-58 interacts with ATGL and potently activates this TAG lipase (21, 29, 38). In fact, addition of CGI-58 to ATGL containing extracts enhances TAG hydrolase activity by ~20-fold (29). The current literature suggests that in lean rodents ATGL and HSL are the major lipases for TAG and DAG, respectively, and account for ~95% of lipase activity in murine WAT (38). Therefore, these molecular steps that regulate lipolysis can be potentially affected by obesity and also be distinctly regulated in VC versus SC WAT. However, very little is known about how diet-induced obesity affects HSL and ATGL content/activity as well as basal and catecholamine-induced lipolysis in VC and SC WAT. Furthermore, although AMPK has been implicated in playing a role in regulating HSL and ATGL activity (3, 17, 20), its action on these major lipases has not been addressed in WAT under diet-induced obesity. Therefore, the present study was designed to address the effects of HFD-induced obesity on lipid metabolism within the adipocyte, specifically the roles of AMPK, HSL, and ATGL in subcutaneous and visceral fat depots. Evidence is provided that dysregulation of lipolysis and lipid metabolism in VC and SC adipocytes of high-fat diet mice is mediated by defective adrenergic receptor signaling combined with upregulation of ATGL and suppression of HSL and AMPK signaling. These findings give new insight into the importance of depot-specific regulation of lipolysis and also address the molecular mechanisms underlying dysfunctional adaptations that occur within the adipocyte with respect to lipid metabolism under conditions of diet-induced obesity and insulin resistance.

## MATERIALS AND METHODS

**Reagents.** Epinephrine, FA-free bovine serum albumin (BSA), free glycerol determination kit, glucose oxidase kit, palmitic acid, and phenylethylamine were obtained from Sigma. [1-<sup>14</sup>C]palmitic acid was from GE Healthcare Radiochemicals (Quebec City, Quebec, Canada). [ $\gamma$ -<sup>32</sup>P]ATP and [9,10-<sup>3</sup>H]triolein were from American Radiolabeled Chemicals (St. Louis, MO). RNeasy Lipid Extraction Kit was from Qiagen. Superscript II and Taq polymerase were from Bio-Rad Canada. DNase kit was from Ambion. Standard and high-fat chow was obtained from LabDiets (Richmond, IN). All antibodies were from Cell Signaling Technology (Beverly, MA) unless otherwise noted. Specific antibodies against phospho-acetyl-CoA carboxylase phosphorylation (ACC) was from Upstate (Charlottesville, VA). Perilipin was from American Research Products (Belmont, MA). All other chemicals were of the highest grade available.

**Animals and isolation of primary adipocytes.** Eight-week-old C57BL/6J male mice were maintained on a 12:12-h light/dark cycle at

22°C and fed ad libitum a standard laboratory chow for a 1-wk acclimation period. Subsequently, the animals were randomly assigned to two groups: control and HFD. Control animals received a standard chow diet containing 25% of kilocalories from fat (TestDiet; LabDiet Cat no. 5015), whereas the HFD group was fed a diet containing 60% of kilocalories from fat (TestDiet; LabDiet Cat no. 58Y1) for 8 wk. A standard chow diet was used for the purpose of comparing the effects of a HFD with those mice fed a diet that supports normal growth and development. The inguinal and epididymal fat pads were used as representative of SC and VC WAT. After the 8-wk study period, SC and VC fat pads were carefully removed and used for adipocyte isolation as previously described (36) with minor modifications (18). Briefly, VC and SC fat pads from control and HFD animals were extracted, weighed, then finely and carefully minced using microscissors. The minced tissue was transferred to plastic vials containing Krebs-Ringer buffer (KRB) supplemented with 30 mM HEPES and collagenase (0.5 g/ml). Tissue was incubated for 25–30 min at 37°C with gentle agitation (120 orbital strokes/min). Subsequently, digested tissue was filtered through a nylon mesh, and cells were collected into plastic 50-ml tubes. Cells were carefully washed three times with collagenase-free KRB-HEPES supplemented with 3.5% BSA (KRBH-3.5% BSA), resuspended in KRBH-3.5% BSA, and allowed to equilibrate for 30 min before use in experiments. The procedures described herein have been adopted to prevent adipocyte lysis and to obtain fat cells that are viable and responsive to stimulation. This is confirmed by ~30- to 40-fold increases in control cells exposed to epinephrine. To distribute equal number of adipocytes in all treatment conditions, cell diameters and numbers were measured as described by DiGirolamo and Fine (13). The experimental protocol was approved by the York University Animal Care Ethics Committee.

**Plasma measurements.** Blood was collected from mice in a fed state at the end of the 8-wk study period and quickly centrifuged at 4°C for 10 min. The serum fraction was collected and stored at –80°C for later analysis. Glucose was measured by using the glucose oxidase kit from Sigma, and nonesterified FAs (NEFAs) were measured by using a kit from Wako Chemicals. Plasma insulin was measured by using an ELISA kit from Millipore.

**Determination of lipolysis, palmitate oxidation, uptake, and incorporation into triacylglycerols.** Lipolysis was determined after adipocytes ( $1 \times 10^5$  cells) had been incubated with constant agitation (80 orbital strokes/min) for 75 min in the absence or presence of epinephrine (100 nM) or forskolin (10  $\mu$ M) (3). For experiments using the EP3 receptor antagonist L826266, cells were preincubated with 10  $\mu$ M of the inhibitor for 2 h before stimulation with epinephrine. After incubation, an aliquot of the media (400  $\mu$ l) was collected and analyzed for glycerol release. The oxidation of palmitate by isolated adipocytes ( $\sim 1 \times 10^6$  cells) was measured in KRBH containing 4% BSA in the presence of 0.2 mM palmitic acid and 0.2  $\mu$ Ci/ml of labeled [1-<sup>14</sup>C]palmitic acid for 1 h. The <sup>14</sup>CO<sub>2</sub> liberated was collected for measurement of oxidation, and lipids were extracted from the cells to measure incorporation of palmitate into TAGs (17, 18). For measurement of palmitate uptake, fat cells ( $1 \times 10^3$ ) were incubated for 20 min in the absence or presence of insulin (100 nM) and subsequently assayed for palmitic acid uptake as described previously (17, 18).

**Citrate synthase activity.** Citrate synthase activity was assayed with adaptations to the method described by Alp et al. (1). Adipose tissue was homogenized in buffer (25 mM Tris-HCl, 1 mM EDTA, pH 7.4) and centrifuged, and the infranant was collected. An aliquot containing 20  $\mu$ g of protein was added to the assay buffer (50 mM Tris-HCl, pH 8.1, 0.2 mM DTNB, 0.1 mM acetyl-CoA, 0.5 mM oxaloacetate), and absorbance was measured over 15 min in a spectrophotometer at 412 nm. The assay control contained all components except the sample, and its value was subtracted from all conditions.

**Quantitative PCR analysis.** Total RNA was isolated from adipocytes using the RNeasy kit, followed by DNase treatment to remove

Table 1. *Body weight, fat mass, and adipocyte diameter*

Diet	Body Weight, g		Fat Pad Mass, g		Adipocyte Diameter, $\mu\text{m}$	
	Baseline	8 Wk	Epididymal	Inguinal	Epididymal	Inguinal
Control	22.7 $\pm$ 0.7	26.1 $\pm$ 0.7	0.84 $\pm$ 0.10	0.25 $\pm$ 0.03	79.4 $\pm$ 2.8	75.5 $\pm$ 4.4
High fat	23.1 $\pm$ 0.6	35.4 $\pm$ 1.2*	2.55 $\pm$ 0.10*	0.70 $\pm$ 0.08*	133.0 $\pm$ 6.3*	119.9 $\pm$ 8.3*

Epididymal and inguinal fat pads were extracted and used as representative tissues for visceral and subcutaneous fat depots. Body weight and fat pad mass were calculated from  $n = 40$  to 45 mice per group. Values are means  $\pm$  SE. Adipocyte diameter was calculated from  $n = 10$ –14. Unpaired  $t$ -tests were used for statistical analyses. \* $P < 0.05$  indicates significance between control versus high fat for that variable.

genomic DNA carryover. The iScript cDNA Synthesis Kit from Bio-Rad Canada was used to prepare cDNA for use in real-time PCR. Primers were designed using the software PrimerQuest (IDT) based on probe sequences available at the Affymetrix database (NetAffx Analysis Center, <http://www.affymetrix.com/analysis>) for each given gene. Real-time PCR reactions were carried out at amplification conditions as follows: 95°C (3 min); 40 cycles of 95°C (10 s), 65°C (15 s), 72°C (30 s); 95°C (15 s), 60°C (15 s), 95°C (15 s). Quantitative PCR was performed using the Bio-Rad CFX96 Real-Time Detection System. All genes were normalized to  $\beta$ -actin and GAPDH as control genes, and values are expressed as fold increases relative to the control diet. Primers sequences are shown in Table 3.

**Western blot analysis.** For whole tissue samples, fat depots were extracted and immediately snap frozen in liquid nitrogen. Tissue (~100 mg) was subsequently homogenized in a buffer composed of 25 mM Tris-HCl and 25 mM NaCl (pH 7.4), 1 mM MgCl<sub>2</sub>, 2.7 mM KCl, and protease and phosphatase inhibitors (0.5 mM Na<sub>3</sub>VO<sub>4</sub>, 1 mM NaF, 1  $\mu\text{M}$  leupeptin, 1  $\mu\text{M}$  pepstatin, 1  $\mu\text{M}$  okadaic acid, and 20 mM PMSF). For isolated adipocytes, cells were stimulated with forskolin (10  $\mu\text{M}$ ) or epinephrine (100 nM) for 30 min before lysis with buffer as described above. To ensure sufficient solubilization of lipid droplet-associated proteins under basal and stimulated conditions, we validated our protein extraction protocol by using an alternative buffer (1% SDS, 1 mM EDTA, 1 mM benzamide, 20 mM NaF, and protease and phosphatase inhibitors) for adipocyte protein extraction and achieved similar results under adrenergic stimulation. Homogenates and lysates were centrifuged, the infranant was collected, and an aliquot was used to measure protein by the Bradford method. Samples were diluted 1:1 (vol/vol) with 2 $\times$  Laemmli buffer, heated to 95°C, and subjected to SDS-PAGE conditions (18). All primary antibodies were used in a dilution of 1:1,000 with the exception of phospho-AMPK (1:500) and perilipin (1:2,000).

**Diacylglycerol content and triacylglycerol lipase activity.** Diacylglycerol (DAG) levels were quantified by a modified enzymatic method (34). Briefly, 100 mg fat tissue from control and HFD mice was homogenized, and lipids were extracted by the method of Bligh and Dyer (8). Once lipids were dried under N<sub>2</sub> gas, DAG content was assessed as previously described by our lab (17). TAG lipase activity was measured as established by Fredrikson et al. (16, 17) and previously performed in our laboratory. Briefly, tissues were homogenized in 2 vol of homogenization buffer and centrifuged for 45 min (4°C, 11,000 g). An aliquot of 100  $\mu\text{g}$  of the protein-rich infranant

Table 2. *Plasma levels of NEFAs, glucose, and insulin from mice in a fed state*

	Control	High Fat
NEFAs, mM	0.39 $\pm$ 0.02	0.53 $\pm$ 0.04*
Glucose, mM	14.35 $\pm$ 0.25	16.23 $\pm$ 0.73*
Insulin, ng/ml	2.55 $\pm$ 0.18	5.76 $\pm$ 0.97*

Data for nonesterified fatty acids (NEFAs), glucose, and insulin were compiled from 36 to 40 mice per condition. Values are means  $\pm$  SE. Unpaired  $t$ -tests were used for statistical analyses. \* $P < 0.05$  indicates significance between control versus high fat for that variable.

was incubated with assay buffer containing a final concentration of 5 mM unlabeled triolein and 0.5  $\mu\text{Ci/ml}$  of labeled [9,10-<sup>3</sup>H]triolein at 37°C for 10 min. The reaction was terminated with the addition of 3.25 ml of extraction buffer and 1.05 ml of a 0.1 M K<sub>2</sub>CO<sub>3</sub>, 0.1 M boric acid solution. Tubes were centrifuged (800 g), and 1 ml from the upper phase containing the liberated [1-<sup>14</sup>C]oleic acid was extracted and counted for radioactivity.

**Statistical analysis.** Data are expressed as means  $\pm$  SE. Statistical significance was set to  $P < 0.05$  and was calculated by using either  $t$ -test or analysis of variance (ANOVA) with Tukey-Kramer post hoc comparisons. The statistical analyses performed for each data set are noted in the figure legends.

## RESULTS

**Body mass, fat mass, adipocyte diameter, and plasma measurements.** Mice in the HFD group had an average of 36% greater body mass than control animals, which was accompanied by an increase of 3.0- and 2.8-fold in epididymal and inguinal fat pad mass, respectively (Table 1). This was compatible with a 1.67- and 1.59-fold increase in adipocyte diameters from the epididymal and inguinal fat pads from the HFD group, respectively (Table 1). When compared with control mice, the HFD group

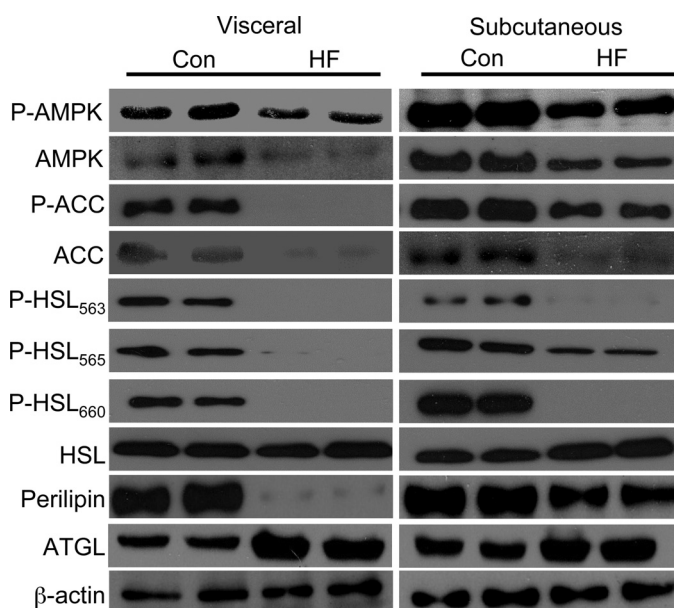


Fig. 1. Phosphorylation of AMP kinase (AMPK), acetyl-CoA carboxylase (ACC), and hormone-sensitive lipase (HSL), and protein content of AMPK, ACC, HSL, perilipin, and adipose triglyceride lipase (ATGL) in white adipose tissue (WAT). After 8 wk on either control (Con) or high-fat (HF) diet, visceral (VC) and subcutaneous (SC) fat depots were extracted and processed for Western blot analysis.  $\beta$ -Actin was used as a loading control. Blots are representative of  $n = 4$ –6 for each condition.

had significantly higher plasma levels of NEFAs, glucose, and insulin (1.36-, 1.13-, and 2.26-fold, respectively), indicating that these animals were an appropriate model for diet-induced obesity and insulin resistance (Table 2).

**Effects of HFD on HSL, AMPK, and ACC phosphorylation and protein content of AMPK, ACC, HSL, ATGL, and perilipin in WAT.** To assess the effects of HFD on major molecular mechanisms that regulate lipolysis in WAT, we examined phosphorylation of HSL on key serine residues as well as the protein content of ATGL and perilipin. Since AMPK has also been implicated in the regulation of HSL activity, the phosphorylation and content of this kinase and of its direct substrate ACC were determined. Phosphorylation of HSL at serine-563, -565, and -660 revealed that these variables were potently suppressed in the VC and SC adipose tissue of HFD mice, despite no change in total HSL protein content (Fig. 1). Perilipin was decreased in both fat depots of HFD mice, although this effect was more pronounced in VC compared with SC adipose tissue. Conversely, the content of ATGL was markedly increased in both fat depots (Fig. 1). Phosphorylation and content of AMPK and ACC was reduced in the VC and SC adipose tissue of HFD mice relative to control animals (Fig. 1).

**DAG content and TAG lipase activity in VC and SC fat depots.** Since HSL phosphorylation was suppressed in VC and SC adipose tissue, we looked at DAG content and TAG lipase activity in these fat depots from control and HFD mice. DAG content increased by 2.5-fold in VC (Fig. 2A) and by 2.9-fold in SC (Fig. 2B) fat pads from HFD mice. TAG lipase activity increased by 1.4- and 2-fold in VC and SC WAT from HF diet mice, respectively (Fig. 2C).

**Lipolysis and phosphorylation of AMPK, ACC, and HSL in VC and SC adipocytes exposed to forskolin and epinephrine.**

As expected, adipocytes from control mice exposed to epinephrine increased glycerol release from  $0.52 \pm 0.04$  to  $14.16 \pm 0.44$  nmol·75 min<sup>-1</sup>·10<sup>-5</sup> cells and from  $0.26 \pm 0.03$  to  $10.49 \pm 1.12$  nmol·75 min<sup>-1</sup>·10<sup>-5</sup> cells in VC and SC adipocytes, respectively (Fig. 3, B and C). When treated with forskolin, glycerol release from VC and SC adipocytes of control mice reached  $12.82 \pm 0.48$  and  $15.61 \pm 1.02$  nmol·75 min<sup>-1</sup>·10<sup>-5</sup> cells, respectively (Fig. 3, B and C). HFD mice had increased basal lipolysis in VC and SC adipocytes by 2.3- and 2.9-fold, respectively, whereas epinephrine-stimulated lipolysis was blunted in both fat depots of HFD animals (Fig. 3, B and C). Treatment of HFD VC adipocytes with forskolin increased lipolysis to levels above

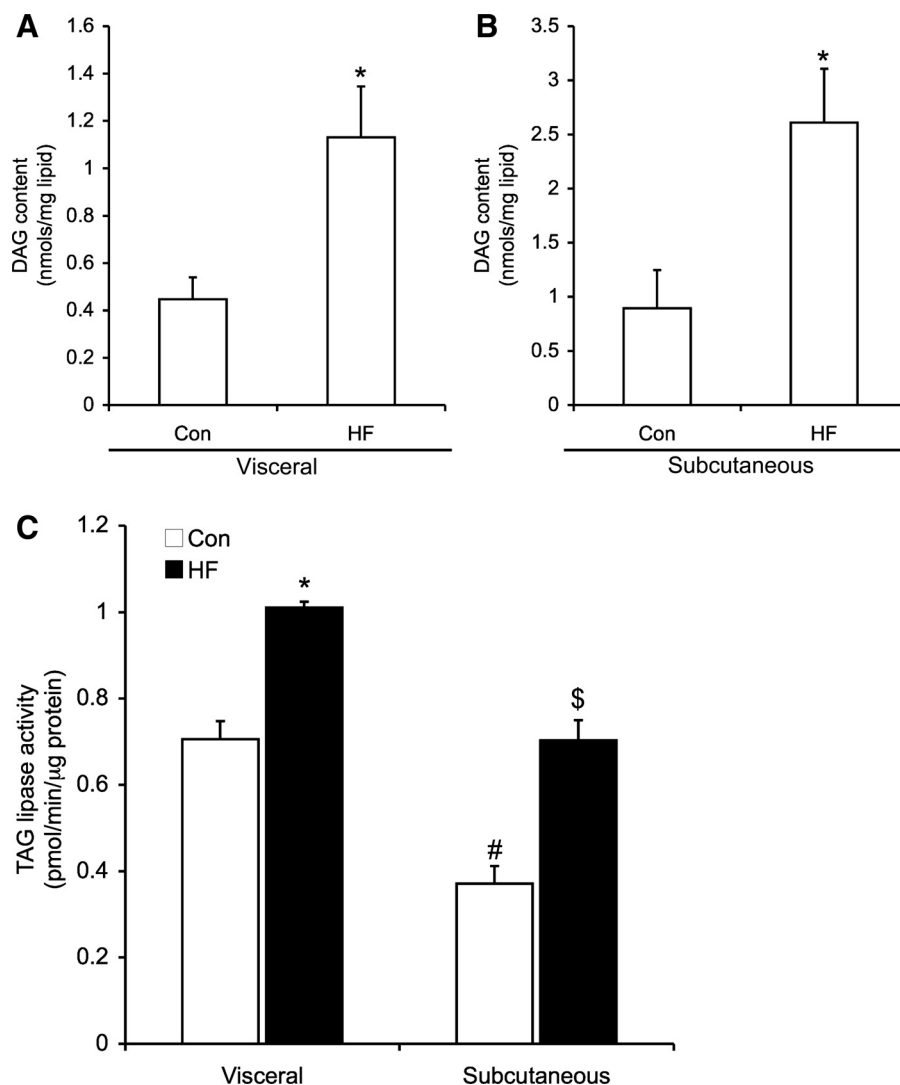


Fig. 2. Diacylglycerol (DAG) content in VC (A) and SC (B) adipose tissues from Con and HF diet mice for 8 wk. Triacylglycerol (TAG) lipase activity in adipose tissue from Con and HF diet mice (C). Data were compiled from 4 to 6 mice from each condition. Unpaired *t*-test or two-way ANOVA with Tukey-Kramer post hoc test was used for statistical analyses. \**P* < 0.05 versus all other conditions; #*P* < 0.05 versus all other conditions; \$*P* < 0.05 versus all other conditions.

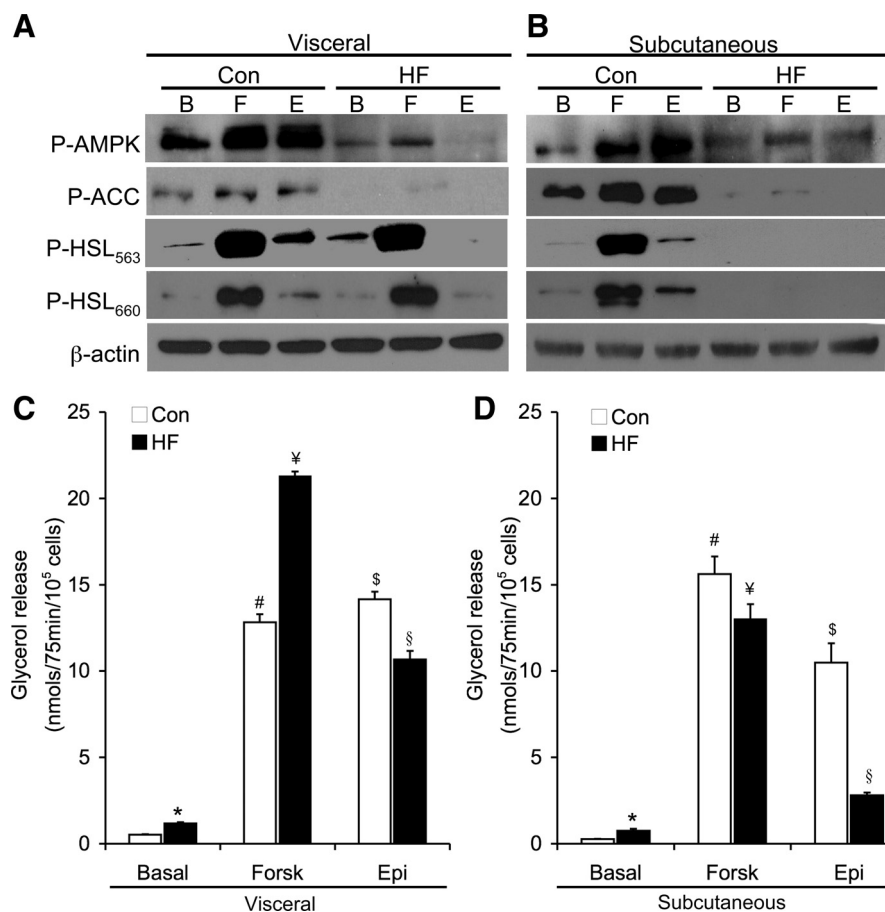


Fig. 3. Determination of AMPK, ACC, and HSL<sub>Ser563/660</sub> phosphorylation under basal (B; vehicle), forskolin (F; 10  $\mu$ M), and epinephrine (E; 100 nM) conditions in VC (A) and SC (B) adipocytes from Con and HF diet mice. Blots are representative of 3 independent experiments. Glycerol release was measured under basal, forskolin (Forsk), and epinephrine (Epi)-stimulated conditions in VC (C) and SC (D) adipocytes from Con and HF mice. Data compiled from 3 independent experiments with quadruplicates for each condition. Two-way ANOVAs were used for statistical analyses. \* $P < 0.05$  versus all other conditions; # $P < 0.05$  versus all other conditions; § $P < 0.05$  versus all other conditions; ¥ $P < 0.05$  versus all other conditions.

those of control VC adipocytes (Fig. 3B); however, only 83% of the lipolytic response was recovered in HFD subcutaneous cells by this agent (Fig. 3C). To assess the potential mechanisms by which HFD induced these alterations in lipolysis, we looked at key proteins involved in the regulation of this pathway. As expected, phosphorylation of AMPK, ACC, and HSL serine-563 and -660 in VC and SC adipocytes from control mice was increased in response to forskolin and epinephrine (Fig. 3A). In HFD VC adipocytes, forskolin- and epinephrine-induced phosphorylation of AMPK and ACC was blunted. Although forskolin was able to increase HSL<sub>Ser563/660</sub> phosphorylation back to control levels, the epinephrine effect on this variable remained suppressed in HFD VC adipocytes (Fig. 3A). In HFD SC fat cells, phosphorylation of AMPK and ACC in response to forskolin and epinephrine was also impaired. Furthermore, contrary to observations in VC adipocytes, phosphorylation of HSL in SC fat cells of the HFD mice was so low that it could not be detected by Western blot analysis under basal, forskolin-, or epinephrine-stimulated conditions (Fig. 3A), despite the fact that total HSL content was unaltered and these cells elicited a significant lipolytic response when exposed to these agents (Fig. 3C).

**Effects of the specific EP3 receptor inhibitor L826266 on VC and SC adipocyte lipolysis.** In an attempt to unravel the mechanisms by which HSL was inhibited under basal and epinephrine-stimulated conditions, we blocked the E-prostanoid 3 (EP3) receptor with the drug L826266 in both VC and SC adipocytes from control and HFD mice. The EP3 receptor

inhibitor increased basal lipolysis from  $0.52 \pm 0.04$  to  $0.97 \pm 0.10$  nmol·75 min<sup>-1</sup>·10<sup>5</sup> cells and from  $0.26 \pm 0.03$  to  $1.60 \pm 0.27$  nmol·75 min<sup>-1</sup>·10<sup>5</sup> cells in VC and SC adipocytes from control animals, respectively. However, it did not affect basal lipolysis in VC ( $1.18 \pm 0.07$  to  $1.48 \pm 0.14$  nmol·75 min<sup>-1</sup>·10<sup>5</sup> cells) and SC ( $0.76 \pm 0.11$  to  $0.72 \pm 0.09$  nmol·75 min<sup>-1</sup>·10<sup>5</sup> cells) adipocytes from HFD animals. Similarly, L826266 did not have any effect on the epinephrine response from VC and SC adipocytes from either control or HFD mice.

**Effect of HFD on palmitate uptake, incorporation into triacylglycerols, oxidation, and citrate synthase activity.** Since TAG breakdown was defective with HFD and was differentially regulated in VC versus SC adipocytes, we also assessed whether parameters involved in lipid metabolism were altered in both fat depots. As expected, insulin elicited a 1.4-fold increase in palmitate uptake by VC adipocytes from control mice (Fig. 4A). However, palmitate uptake by VC adipocytes from HFD mice decreased by 26% and 37% under basal and insulin-stimulated conditions relative to control VC adipocytes, respectively (Fig. 4A). In SC adipocytes from HFD mice, suppression in both basal and insulin-stimulated palmitate uptake (17% and 28%, respectively) was also observed compared with control SC fat cells. Despite a reduction in palmitate uptake, palmitate incorporation into TAGs increased above controls by 1.7-fold in VC (Fig. 4C) and by 1.5-fold in SC (Fig. 4D) adipocytes from HFD mice. Palmitate oxidation was decreased in both VC and SC adipocytes from HFD mice by ~64% and 75%, respectively (Fig. 5, A and B). In line with these changes,

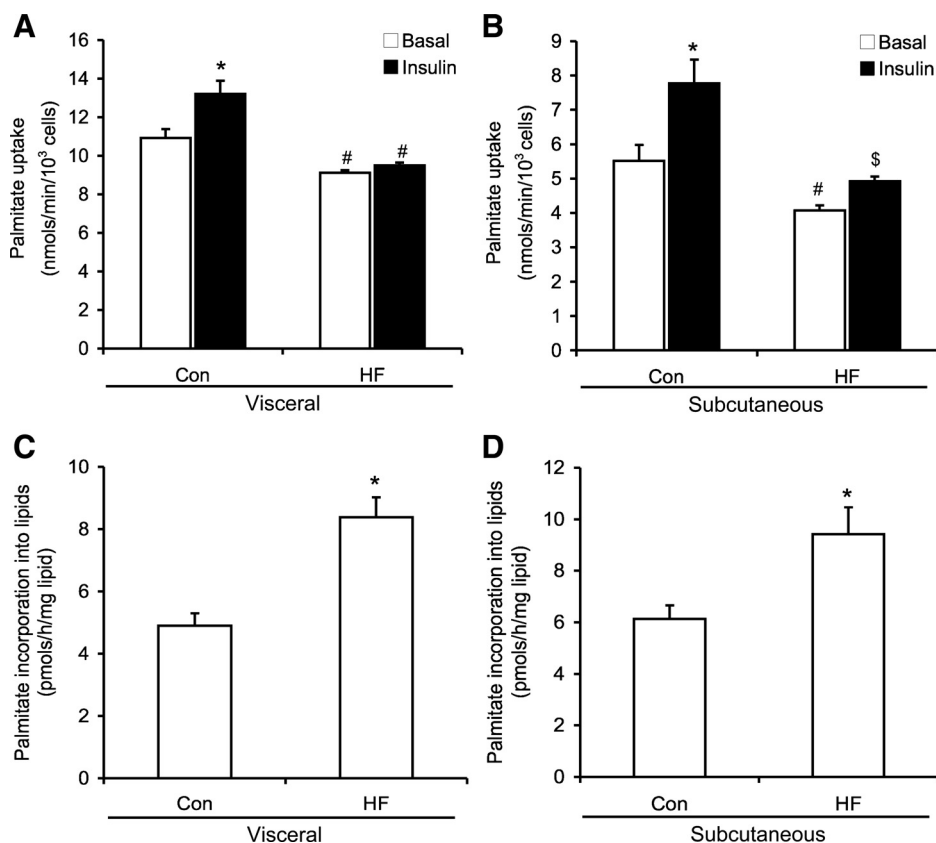


Fig. 4. Palmitate uptake in VC (A) and SC (B) adipocytes isolated from Con and mice on a HF diet for 8 wk under basal and insulin-stimulated conditions and palmitate incorporation into lipids in VC (C) and SC (D) fat cells. Data were compiled from 2 to 3 independent experiments, with triplicates for each condition. Two-way ANOVAs or unpaired *t*-tests were used for statistical analyses. \**P* < 0.05 versus Con; #*P* < 0.05 versus all other conditions; \$*P* < 0.05 versus Con basal and Con insulin-stimulated conditions.

citrate synthase activity was also reduced by 46% in VC and by 63% in SC adipocytes from HFD mice (Fig. 5C).

**Analysis of gene expression in VC and SC fat depots by quantitative PCR.** We utilized quantitative PCR to determine whether the expression of genes involved in the regulation of lipolysis and lipid metabolism were altered in VC and SC adipose tissue from HFD mice. The mRNA levels of the  $\alpha$ 1-isoform of AMPK were decreased in VC and SC adipose tissue from HFD compared with control animals, whereas the expression of the  $\alpha$ 2-isoform remained unchanged (Table 3). Additionally, mRNA levels of other proteins involved in oxidative metabolism such as ACC $\alpha$ , cytochrome-*c* oxidase subunit VIII (Cox8), peroxisome proliferator-activated receptor- $\alpha$  (PPAR $\alpha$ ), and PGC-1 $\alpha$  were decreased in both VC (~57, 67, 72, and 57%, respectively) and SC (~43, 73, 52, and 54%, respectively) adipose tissues from HFD mice (Table 3). Expression of CGI-58 was significantly upregulated in both fat depots reaching 1.7-fold in VC and 1.8-fold in SC adipose tissues of HFD mice. The expression of adipose phospholipase A<sub>2</sub> (AdPLA<sub>2</sub>) in VC and SC adipose tissues was significantly increased with HFD by 1.9- and 2.3-fold compared with control mice, respectively.

## DISCUSSION

Here, we provide novel evidence that the increased basal but blunted epinephrine-stimulated lipolysis with HFD-induced obesity is mediated by impaired adrenergic receptor signaling, suppression of HSL phosphorylation, and upregulation of ATGL content and CGI-58 expression. Phosphorylation of HSL at serine residues 563 and 660, which is required for PKA-

mediated lipolysis (2), was potently suppressed by HFD in both VC and SC fat tissues. Since ATGL functions essentially as a TAG lipase (38, 47), upregulation of ATGL content in combination with increased expression of its coactivator CGI-58 must have promoted TAG breakdown and formation of DAG. This is supported by our data indicating that TAG lipase activity is increased in WAT from HFD mice. Conversely, HFD-induced suppression of HSL phosphorylation/activity impaired breakdown of DAG, thereby facilitating its accumulation in the WAT. This is evidenced by our findings that DAG content was significantly increased by 2.5- and 2.9-fold in VC and SC WAT, respectively. This is also in line with previous studies in HSL knockout mice showing that in the absence of this lipase, accumulation of DAG in WAT occurs (23).

Bypassing the adrenergic-receptor-mediated activation of adenylyl cyclases with forskolin fully rescued HFD-induced suppression of HSL phosphorylation at serine-563 and -660 residues in visceral adipocytes. Interestingly, in HFD subcutaneous adipocytes, lipolysis was partially rescued by forskolin and this occurred in the absence of any detectable induction of HSL phosphorylation. Studies in HSL-null mice show residual lipolysis, indicating that this process is impaired by the lack HSL activity, although not entirely dependent on this lipase. Studies from other labs support these findings, where silencing HSL using small interfering RNA diminished forskolin-stimulated lipolysis by 53%, whereas knocking down of ATGL resulted in ~90% reduction in glycerol release in differentiated human adipocytes (7). In line with these observations, we found that the ATGL content and the expression of its coactivator CGI-58 were both increased by HFD, which is compat-

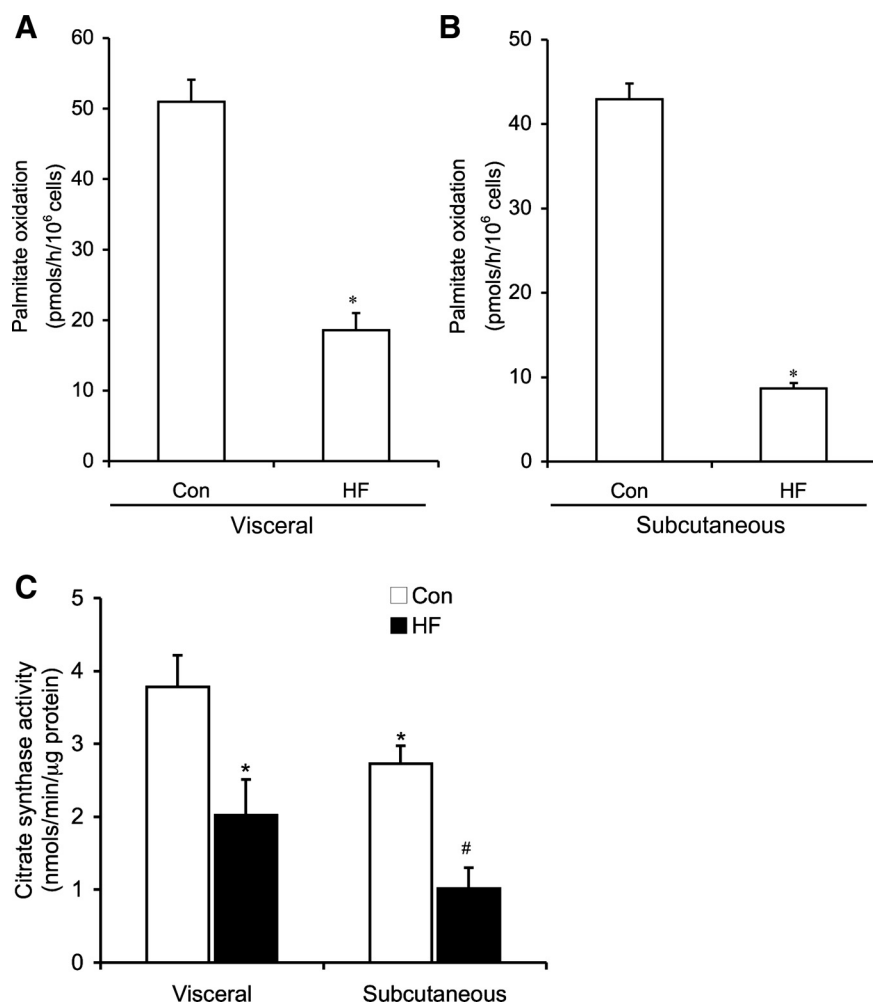


Fig. 5. Palmitate oxidation in VC (A) and SC (B) adipocytes isolated from Con and HFD mice and citrate synthase activity (C). Data are representative of 3 independent experiments, with a minimum of triplicates for each condition. Two-way ANOVA or unpaired *t*-tests were used for statistical analyses. \**P* < 0.05 versus Con; #*P* < 0.05 versus all other conditions.

ible with increased lipolysis in HFD visceral and subcutaneous adipocytes exposed to forskolin. It is important to note that even though forskolin substantially increased lipolysis in HFD subcutaneous adipocytes, it was still limited to ~83% of the values obtained with control cells exposed to this agent. This indicates that although a potent forskolin-induced lipolytic response could be obtained through upregulation of ATGL and CGI-58, the lack of HSL phosphorylation/activation limited the ability of HFD subcutaneous adipocytes to fully respond to this agent. This is further supported by our findings that HSL<sub>Ser563/660</sub> was equally phosphorylated in HFD and control visceral adipocytes exposed to forskolin. Noteworthy, the lipolytic response of HFD adipocytes surpassed (1.67-fold) that of control VC cells treated with forskolin, even though no additional phosphorylation of HSL was observed.

The exposure of VC and SC adipocytes from control and HFD mice to forskolin also demonstrated that signaling steps mediated by adrenergic receptors play an important role in determining the well-characterized differences in lipolytic rates between VC and SC fat depots (4). This is evidenced by the fact that absolute values for lipolysis under basal and epinephrine stimulation in control and HFD VC fat cells were consistently higher than the values obtained with SC adipocytes. However, upon stimulation with forskolin, control SC lipolysis was 1.22-fold higher than in VC control adipocytes. These

findings demonstrate that SC adipocytes have the potential to elicit lipolytic responses that are similar or even higher than those of VC adipocytes, but early signaling steps mediated by activation of adrenergic receptors appear to maintain a lower lipolytic rate in SC adipocytes from lean mice.

Besides HSL phosphorylation, the content of perilipin was also reduced in both fat depots with HFD. In HFD VC WAT perilipin levels were hardly detectable, whereas in SC WAT the content of this protein was less than control, although still abundantly present. Reduced perilipin content has been demonstrated to alter the normal breakdown of neutral lipids in fat cells. In fact, it has previously been reported that basal lipolysis is elevated, whereas isoproterenol-stimulated lipolysis is severely blunted in perilipin null mice (44). Based on these observations, it was proposed that perilipin exerts an important role in preventing lipases from accessing neutral lipid stores under basal conditions, whereas its presence is required for PKA-mediated lipolysis (10, 44). In the absence of adrenergic stimulation, HSL is mainly located in the cytoplasm, whereas perilipin is on the surface of the lipid droplet (43). Upon  $\beta$ -adrenergic stimulation, activated PKA phosphorylates HSL as well as perilipin (31, 41). HSL then translocates to the lipid droplet and colocalizes with perilipin leading to enhancement in hydrolysis of neutral lipids (41, 43, 45), indicating that the interaction of perilipin and HSL is essential for the PKA-

Table 3. *Quantitative PCR analysis of mRNA expression*

Gene	Primer Sequences (5' → 3')	Fold Change Relative to Control Diet	
		VC	SC
AMPK $\alpha$ 1	F-TGACCGGACATAAAGTGGCTGTGA R-TGATGATGTGAGGGTGCCTGAACA	0.45 $\pm$ 0.01*	0.87 $\pm$ 0.03*
AMPK $\alpha$ 2	F-TGGATCGCCAAATTATGCAGCACC R-AAGGGCATAACAGGATGACACCACA	0.70 $\pm$ 0.25	1.01 $\pm$ 0.23
ACC- $\alpha$	F-ACCTTACTGCCATCCCATGTGCTA R-GTGCCTGATGATCGCACGAACAAA	0.43 $\pm$ 0.07*	0.57 $\pm$ 0.05*
Cox 8	F-TCTCAGCCATAGTCGTTGGCTTCA R-CAACTTCATGCTGCGGAGCTCTTT	0.33 $\pm$ 0.01*	0.27 $\pm$ 0.01*
PGC-1 $\alpha$	F-ACCGTAAATCTGCGGGATGATGGA R-AGTCAGTTTCGTTGACCTGCGTA	0.43 $\pm$ 0.07*	0.46 $\pm$ 0.09*
PPAR $\alpha$	F-ATGAAGAGGGCTGAGCGTAGGTAA R-TGCCGTTGTCTGTCACTGTCTGAA	0.28 $\pm$ 0.06*	0.48 $\pm$ 0.02*
CGI-58	F-TGTGCAGGACTCTTACTTGGCAGT R-GTTTCTTTGGGCAGACCGGTTTCT	1.70 $\pm$ 0.15*	1.98 $\pm$ 0.30*
AdPLA <sub>2</sub>	F-ATAACAGTCTTTCCTGGCTGCCCT R-TCCATTTCTGTGTACCCAGGCTGT	1.94 $\pm$ 0.24*	2.28 $\pm$ 0.15*

Values are means  $\pm$  SE. F, forward; R, reverse. Fold changes in visceral (VC) and subcutaneous (SC) adipose tissues from high-fat diet mice relative to control diet. Samples were run in duplicate on the plate, and data were compiled from 3 to 4 separate plates, with  $n = 6-8$  for each condition. GAPDH and  $\beta$ -actin were used as control genes. AMPK, AMP kinase; ACC, acetyl-CoA carboxylase; Cox 8, cytochrome-*c* oxidase subunit VIII; PGC-1 $\alpha$ , proliferator-activated receptor- coactivator-1 $\alpha$ ; PPAR $\alpha$ , peroxisome proliferator-activated receptor- $\alpha$ ; CGI-58, comparative gene identification-58; AdPLA<sub>2</sub>, adipose phospholipase A<sub>2</sub>. Unpaired *t*-tests were used for statistical analyses. \* $P < 0.05$  versus control diet.

mediated effects on lipolysis (10, 32). Our data are consistent with these observations, since the HFD-induced reduction in perilipin content coincided with 3.8- and 3.0-fold increases in basal lipolysis in VC and SC fat cells, respectively, whereas

epinephrine-stimulated lipolysis was equally and potently blunted in HFD adipocytes from both fat depots.

Another pathway that plays an important role in the regulation of lipolysis involves prostaglandins, particularly prosta-

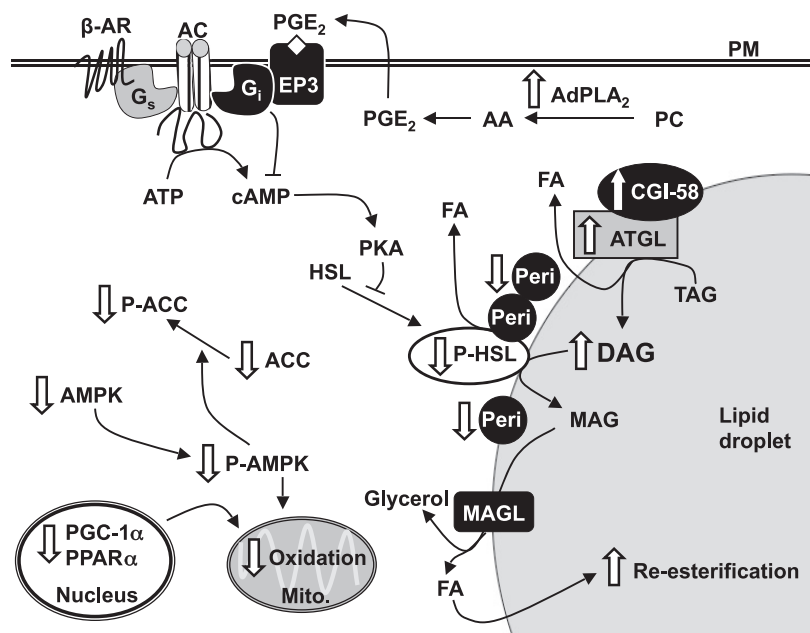


Fig. 6. Summary of the effects of HFD on adipocyte lipolysis and metabolism. Arrows represent up- or downregulation of activity, protein content, and/or expression. Lines without arrowheads denote inhibition. Under HFD, the effect of catecholamines on the  $\beta$ -adrenergic ( $\beta$ -AR) signaling cascade are blunted through reduced activation of the G stimulatory protein coupled receptor ( $G_s$ ). This reduces protein kinase A (PKA) activation and inhibits phosphorylation of hormone-sensitive lipase (HSL). HFD also upregulates expression of adipose tissue phospholipase A<sub>2</sub> (AdPLA<sub>2</sub>), which has been demonstrated to increased prostaglandin E<sub>2</sub> (PGE<sub>2</sub>) production, the primary ligand for the E-prostanoid 3 receptor (EP3). Since EP3 is coupled to an inhibitory G protein ( $G_i$ ), activation of this receptor further inhibits PKA under HFD conditions. Increase in ATGL content and comparative gene identification-58 (CGI-58) expression also occurs with HFD to facilitate TAG breakdown, although subsequent decreased HSL phosphorylation/activity results in the accumulation of DAG. HFD-induced decreases in perilipin (Peri) content also seems to contribute to dysfunctional lipolysis in these cells. Reduction of AMPK content and phosphorylation by HFD is in line with reduced ACC and suppressed oxidation. The oxidative capacity of adipocytes is decreased with HFD, which is compatible with suppression of regulators of mitochondrial biogenesis such as peroxisome proliferator-activated receptor- $\gamma$  (PPAR $\gamma$ ) coactivator-1 $\alpha$  (PGC-1 $\alpha$ ) and PPAR $\alpha$  expression. AC, adenylyl cyclase; AA, arachidonic acid; PC, phosphatidylcholine; PM, plasma membrane; FA, fatty acid; MAG; monoacylglycerol; MAGL, MAG lipase; Mito, mitochondria.

glandin E<sub>2</sub> (PGE<sub>2</sub>). PGE<sub>2</sub> levels are reported to be upregulated in adipose tissue from obese humans and acts on the EP3 receptor that signals through G<sub>i</sub>-coupled protein receptors to reduce intracellular cAMP levels and potently inhibits lipolysis (46). In adipose tissue, PGE<sub>2</sub> is synthesized by adipose phospholipase A<sub>2</sub> (AdPLA<sub>2</sub>) and is secreted by adipocytes (14). It was recently demonstrated that ablation of AdPLA<sub>2</sub> in mice generates a phenotype that prevents obesity induced by HFD and elevates lipolysis, primarily through a decrease in PGE<sub>2</sub> production and content in WAT (24). In the HFD mice, we found a significant increase in AdPLA<sub>2</sub> expression in VC and SC WAT, which is compatible with increased PGE<sub>2</sub> levels seen in obese individuals (14). Therefore, we hypothesized that overactivation of the EP3 receptor due to elevated prostaglandin secretion by HFD adipocytes could be responsible for the impairment in adrenergic receptor signaling and blunted catecholamine-induced lipolysis in VC and SC adipocytes of HFD mice. Preincubation with the EP3 receptor antagonist L826266 increased basal lipolysis in control VC and SC adipocytes. However, it did not alter the potent inhibitory effect of HFD on epinephrine-induced lipolysis. The reasons underlying this are unclear though it could be that after 8 wk of HFD, the EP3 receptor was hyperactivated and acute incubation with L826266 was unable to overcome the powerful suppressive effect of the prolonged HFD on this pathway. It is also important to note that the β<sub>3</sub>-adrenergic receptor is highly expressed in mouse adipose tissue (4, 33) and the use of a selective agonist for this receptor could have elicited a distinct lipolytic response in VC and SC adipocytes of HFD mice. This is particularly important considering that the distribution of β-adrenergic receptor isoforms in WAT differs between rodents and humans (4). Therefore, future investigations utilizing isoform-specific agonists and antagonists of β-adrenergic receptors are warranted to unravel the roles of distinct β-isoforms in lipolysis under conditions of HFD either in the absence or presence of the EP3 receptor antagonist.

Although AMPK activation has been shown to exert an antilipolytic effect in WAT, its effect on metabolic processes under conditions of HFD have not yet been assessed. Here, we provide novel evidence that both phosphorylation and content of AMPK and its substrate ACC were strongly reduced in both VC and SC fat tissue from HFD mice. Although this seems consistent with the fact that basal lipolysis is elevated, HFD completely abolished HSL phosphorylation on PKA targets serine-563 and -660 with a concomitant reduction in AMPK activity. Therefore, the inhibition of catecholamine-induced lipolysis cannot be attributed to exacerbated activation of this kinase by HFD. In fact, lower phosphorylation of ACC and HSL<sub>Ser565</sub>, downstream targets of AMPK (3, 19), is in line with the reduced activation of this kinase in VC and SC fat depots of HFD mice. Furthermore, we have previously demonstrated that short- and long-term 5-aminoimidazole-4-carboxamide-1-β-D-ribofuranoside (AICAR)-induced AMPK activation reduces FA esterification (17, 18). In the present study, we show that a reduction in AMPK signaling with HFD elicits the opposite effect, since FA incorporation into lipids was increased, whereas citrate synthase activity and palmitate oxidation were reduced, which is also compatible with facilitation of lipid storage in a condition of chronic energy surplus. Furthermore, it is fitting that under conditions of HFD the production of citrate is reduced, since the cells are exposed to an abundance of FAs and there is no need for the de novo lipid

synthesis pathway to be activated. HFD not only reduced AMPK phosphorylation but also promoted insulin resistance in both fat depots. This was clearly demonstrated by the fact that insulin-stimulated palmitate uptake was inhibited by HFD in VC and SC adipocytes. In this scenario, impairment of AMPK signaling must have facilitated the release of FAs by the WAT, since the anti-lipolytic effect of this kinase was attenuated.

To date, no studies have demonstrated whether the FA oxidative pathway in adipocytes is altered under conditions of diet-induced obesity. Here, we provide evidence that the oxidative capacity of both VC and SC adipocytes was markedly decreased in fat cells from HFD mice. Although this maybe partly attributed to reduced palmitate uptake in adipocytes of HFD mice, changes in the expression of genes involved in oxidative metabolism were also altered. Gene expression of PGC-1α and PPARα, which are critical regulators of mitochondrial biogenesis and energy expenditure (35), were significantly reduced in both VC and SC WAT. Importantly, it has been recently shown that AMPK and another energy sensor, the NAD<sup>+</sup>-dependent type III deacetylase SIRT1, are necessary for PGC-1α activation (11). Therefore, chronic suppression of AMPK as seen in the WAT of HFD mice is consistent with a reduced ability of this tissue to upregulate oxidative metabolism. Furthermore, recent studies from our lab indicated that AICAR-induced activation of AMPK for 15 h increased gene expression of PGC-1α and PPARα, which drove lipid metabolism toward energy dissipation instead of storage (17). Although the WAT does not have high oxidative capacity, these differences in metabolism of FAs could have a major impact on whole body lipid metabolism, because fat tissue makes up a large proportion of body mass (15–20% and 20–30% in healthy men and women, respectively), particularly in obese individuals (more than 40%) (12). Although there is no evidence that FA oxidation in adipocytes increases as a means to cope with excess lipid load in obesity, our data suggest that the impairment of FA oxidation in WAT may further contribute to the accumulation of fat mass in both visceral and subcutaneous fat depots under conditions of HFD.

In summary, our results indicate that HFD-induced obesity disrupts signaling through major components of the lipolytic cascade in WAT (Fig. 6). Specifically, HSL and perilipin are downregulated, whereas ATGL and CGI-58 are upregulated. This culminates in increased basal but severely blunted catecholamine-induced lipolysis and accumulation of DAG in VC and SC fat depots. Additionally, impairment of AMPK activity and downregulation of PGC-1α and PPARα resulted in elevated esterification and reduced ability to oxidize FA in VC and SC adipocytes (Fig. 6). Altogether, these alterations in molecular regulation of lipolysis and FA metabolism give insight into the dysfunctional metabolic adaptations that occur with HFD in the WAT and may help further our understanding of defective mechanisms that contribute to obesity and its related metabolic disorders.

#### ACKNOWLEDGMENTS

The authors thank Merck Frosst for the kind gift of L826266.

#### GRANTS

This research was funded by an operating grant from the Canadian Institute of Health Research (CIHR) and by infrastructure grants from the Canada Foundation for Innovation (CFI) and the Ontario Research Fund (ORF)

awarded to R. B. Ceddia. R. B. Ceddia is also a recipient of the CIHR New Investigator Award and the Early Research Award from the Ontario Ministry of Research and Innovation. M. P. Gaidhu and N. M. Anthony are supported by Doctoral and Masters CIHR Canadian Graduate Scholarships, respectively.

## DISCLOSURES

The authors state no conflict or duality of interest in regards to this work.

## REFERENCES

- Alp PR, Newsholme EA, Zammit VA. Activities of citrate synthase and NAD<sup>+</sup>-linked and NADP<sup>+</sup>-linked isocitrate dehydrogenase in muscle from vertebrates and invertebrates. *Biochem J* 154: 689–700, 1976.
- Anthonsen MW, Ronnstrand L, Wernstedt C, Degerman E, Holm C. Identification of novel phosphorylation sites in hormone-sensitive lipase that are phosphorylated in response to isoproterenol and govern activation properties in vitro. *J Biol Chem* 273: 215–221, 1998.
- Anthony NM, Gaidhu MP, Ceddia RB. Regulation of visceral and subcutaneous adipocyte lipolysis by acute AICAR-induced AMPK activation. *Obesity* 17: 1312–1317, 2009.
- Arner P. Human fat cell lipolysis: biochemistry, regulation and clinical role. *Best Pract Res Clin Endocrinol Metab* 19: 471–482, 2005.
- Bays HE, Gonzalez-Campoy JM, Bray GA, Kitabchi AE, Bergman DA, Schorr AB, Rodbard HW, Henry RR. Pathogenic potential of adipose tissue and metabolic consequences of adipocyte hypertrophy and increased visceral adiposity. *Expert Rev Cardiovasc Ther* 6: 343–368, 2008.
- Bergman RN, Kim SP, Hsu IR, Catalano KJ, Chiu JD, Kabir M, Richey JM, Ader M. Abdominal obesity: role in the pathophysiology of metabolic disease and cardiovascular risk. *Am J Med* 120: S3–S8; discussion S29–S32, 2007.
- Bezair V, Mairal A, Ribet C, Lefort C, Girousse A, Jocken J, Laurencikienė J, Anesia R, Rodriguez AM, Ryden M, Stenson BM, Dani C, Ailhaud G, Arner P, Langin D. Contribution of adipose triglyceride lipase and hormone-sensitive lipase to lipolysis in human hMADS adipocytes. *J Biol Chem* 284: 18282–18291, 2009.
- Bligh EG, Dyer WJ. A rapid method of total lipid extraction and purification. *Can J Biochem Physiol* 37: 911–917, 1959.
- Bolinder J, Kager L, Ostman J, Arner P. Differences at the receptor and postreceptor levels between human omental and subcutaneous adipose tissue in the action of insulin on lipolysis. *Diabetes* 32: 117–123, 1983.
- Brasaemle DL. Thematic review series: adipocyte biology. The perilipin family of structural lipid droplet proteins: stabilization of lipid droplets and control of lipolysis. *J Lipid Res* 48: 2547–2559, 2007.
- Canto C, Gerhart-Hines Z, Feige JN, Lagouge M, Noriega L, Milne JC, Elliott PJ, Puigserver P, Auwerx J. AMPK regulates energy expenditure by modulating NAD<sup>+</sup> metabolism and SIRT1 activity. *Nature* 458: 1056–1060, 2009.
- Ceddia RB. Direct metabolic regulation in skeletal muscle and fat tissue by leptin: implications for glucose and fatty acids homeostasis. *Int J Obes (Lond)* 29: 1175–1183, 2005.
- DiGirolamo M, Fine JB. Cellularity measurements. *Methods Mol Biol* 155: 65–75, 2001.
- Fain JN, Madan AK, Hiler ML, Cheema P, Bahouth SW. Comparison of the release of adipokines by adipose tissue, adipose tissue matrix, and adipocytes from visceral and subcutaneous abdominal adipose tissues of obese humans. *Endocrinology* 145: 2273–2282, 2004.
- Frayn KN, Karpe F, Fielding BA, Macdonald IA, Coppack SW. Integrative physiology of human adipose tissue. *Int J Obes Relat Metab Disord* 27: 875–888, 2003.
- Fredrikson G, Stralfors P, Nilsson NO, Belfrage P. Hormone-sensitive lipase from adipose tissue of rat. *Methods Enzymol* 71: 636–646, 1981.
- Gaidhu MP, Fediuc S, Anthony NM, So M, Mirpourian M, Perry RL, Ceddia RB. Prolonged AICAR-induced AMP-kinase activation promotes energy dissipation in white adipocytes: novel mechanisms integrating HSL and ATGL. *J Lipid Res* 50: 704–715, 2009.
- Gaidhu MP, Fediuc S, Ceddia RB. 5-Aminoimidazole-4-carboxamide-1-beta-D-ribofuranoside-induced AMP-activated protein kinase phosphorylation inhibits basal and insulin-stimulated glucose uptake, lipid synthesis, and fatty acid oxidation in isolated rat adipocytes. *J Biol Chem* 281: 25956–25964, 2006.
- Garton AJ, Campbell DG, Carling D, Hardie DG, Colbran RJ, Yeaman SJ. Phosphorylation of bovine hormone-sensitive lipase by the AMP-activated protein kinase. A possible antilipolytic mechanism. *Eur J Biochem* 179: 249–254, 1989.
- Gauthier MS, Miyoshi H, Souza SC, Cacicedo JM, Saha AK, Greenberg AS, Ruderman NB. AMP-activated protein kinase is activated as a consequence of lipolysis in the adipocyte: potential mechanism and physiological relevance. *J Biol Chem* 283: 16514–16524, 2008.
- Granneman JG, Moore HP, Granneman RL, Greenberg AS, Obin MS, Zhu Z. Analysis of lipolytic protein trafficking and interactions in adipocytes. *J Biol Chem* 282: 5726–5735, 2007.
- Granneman JG, Moore HP, Krishnamoorthy R, Rathod M. Perilipin controls lipolysis by regulating the interactions of ab-hydrolase containing 5 (Abhd5) and adipose triglyceride lipase (ATGL). *J Biol Chem* 284: 34538–34544, 2009.
- Haemmerle G, Zimmermann R, Hayn M, Theussl C, Waeg G, Wagner E, Sattler W, Magin TM, Wagner EF, Zechner R. Hormone-sensitive lipase deficiency in mice causes diglyceride accumulation in adipose tissue, muscle, and testis. *J Biol Chem* 277: 4806–4815, 2002.
- Jaworski K, Ahmadian M, Duncan RE, Sarkadi-Nagy E, Varady KA, Hellerstein MK, Lee HY, Samuel VT, Shulman GI, Kim KH, de Val S, Kang C, Sul HS. AdPLA ablation increases lipolysis and prevents obesity induced by high-fat feeding or leptin deficiency. *Nat Med* 15: 159–168, 2009.
- Jensen MD. Role of body fat distribution and the metabolic complications of obesity. *J Clin Endocrinol Metab* 93: S57–S63, 2008.
- Jocken JW, Blaak EE. Catecholamine-induced lipolysis in adipose tissue and skeletal muscle in obesity. *Physiol Behav* 94: 219–230, 2008.
- Lafontan M, Langin D. Lipolysis and lipid mobilization in human adipose tissue. *Prog Lipid Res* 48: 275–297, 2009.
- Large V, Arner P. Regulation of lipolysis in humans. Pathophysiological modulation in obesity, diabetes, and hyperlipidaemia. *Diabetes Metab* 24: 409–418, 1998.
- Lass A, Zimmermann R, Haemmerle G, Riederer M, Schoiswohl G, Schweiger M, Kienesberger P, Strauss JG, Gorkiewicz G, Zechner R. Adipose triglyceride lipase-mediated lipolysis of cellular fat stores is activated by CGI-58 and defective in Chanarin-Dorfman Syndrome. *Cell Metab* 3: 309–319, 2006.
- Mauriege P, Galitzky J, Berlan M, Lafontan M. Heterogeneous distribution of beta and alpha-2 adrenoceptor binding sites in human fat cells from various fat deposits: functional consequences. *Eur J Clin Invest* 17: 156–165, 1987.
- Miyoshi H, Perfield JWn Souza SC, Shen WJ, Zhang HH, Stancheva ZS, Kraemer FB, Obin MS, Greenberg AS. Control of adipose triglyceride lipase action by serine 517 of perilipin A globally regulates protein kinase A-stimulated lipolysis in adipocytes. *J Biol Chem* 282: 996–1002, 2007.
- Moore HP, Silver RB, Mottillo EP, Bernlohr DA, Granneman JG. Perilipin targets a novel pool of lipid droplets for lipolytic attack by hormone-sensitive lipase. *J Biol Chem* 280: 43109–43120, 2005.
- Nahmias C, Blin N, Elalouf JM, Mattei MG, Strosberg AD, Emorine LJ. Molecular characterization of the mouse beta 3-adrenergic receptor: relationship with the atypical receptor of adipocytes. *EMBO J* 10: 3721–3727, 1991.
- Preiss J, Loomis CR, Bishop WR, Stein R, Nidel JE, Bell RM. Quantitative measurement of sn-1,2-diacylglycerols present in platelets, hepatocytes, and ras- and sis-transformed normal rat kidney cells. *J Biol Chem* 261: 8597–8600, 1986.
- Puigserver P, Wu Z, Park CW, Graves R, Wright M, Spiegelman BM. A cold-inducible coactivator of nuclear receptors linked to adaptive thermogenesis. *Cell* 92: 829–839, 1998.
- Rodbell M. Metabolism of isolated fat cells. I. Effects of hormones on glucose metabolism and lipolysis. *J Biol Chem* 239: 375–380, 1964.
- Roden M. How free fatty acids inhibit glucose utilization in human skeletal muscle. *News Physiol Sci* 19: 92–96, 2004.
- Schweiger M, Schreiber R, Haemmerle G, Lass A, Fledelius C, Jacobsen P, Tornqvist H, Zechner R, Zimmermann R. Adipose triglyceride lipase and hormone-sensitive lipase are the major enzymes in adipose tissue triacylglycerol catabolism. *J Biol Chem* 281: 40236–40241, 2006.
- Shen WJ, Patel S, Natu V, Kraemer FB. Mutational analysis of structural features of rat hormone-sensitive lipase. *Biochemistry* 37: 8973–8979, 1998.
- Stumvoll M, Goldstein BJ, van Haeften TW. Type 2 diabetes: principles of pathogenesis and therapy. *Lancet* 365: 1333–1346, 2005.

41. **Su CL, Sztalryd C, Contreras JA, Holm C, Kimmel AR, Londos C.** Mutational analysis of the hormone-sensitive lipase translocation reaction in adipocytes. *J Biol Chem* 278: 43615–43619, 2003.
42. **Sztalryd C, Kraemer FB.** Differences in hormone-sensitive lipase expression in white adipose tissue from various anatomic locations of the rat. *Metabolism* 43: 241–247, 1994.
43. **Sztalryd C, Xu G, Dorward H, Tansey JT, Contreras JA, Kimmel AR, Londos C.** Perilipin A is essential for the translocation of hormone-sensitive lipase during lipolytic activation. *J Cell Biol* 161: 1093–1103, 2003.
44. **Tansey JT, Sztalryd C, Gruia-Gray J, Roush DL, Zee JV, Gavrilova O, Reitman ML, Deng CX, Li C, Kimmel AR, Londos C.** Perilipin ablation results in a lean mouse with aberrant adipocyte lipolysis, enhanced leptin production, and resistance to diet-induced obesity. *Proc Natl Acad Sci USA* 98: 6494–6499, 2001.
45. **Wang H, Hu L, Dalen K, Dorward H, Marcinkiewicz A, Russel D, Gong D, Londos C, Yamaguchi T, Holm C, Rizzo MA, Brasaemle D, Sztalryd C.** Activation of hormone-sensitive lipase requires two steps: protein phosphorylation and binding to the PAT-1 domain of lipid droplet coat proteins. *J Biol Chem* 284: 32116–32125, 2009.
46. **Wolf G.** Adipose-specific phospholipase as regulator of adiposity. *Nutr Rev* 67: 551–554, 2009.
47. **Zimmermann R, Strauss JG, Haemmerle G, Schoiswohl G, Birner-Gruenberger R, Riederer M, Lass A, Neuberger G, Eisenhaber F, Hermetter A, Zechner R.** Fat mobilization in adipose tissue is promoted by adipose triglyceride lipase. *Science* 306: 1383–1386, 2004.

